# The deprotection reaction front profile in model 193 nm methacrylate-based chemically amplified photoresists[§]

Bryan D. Vogt[a], Shuhui Kang[a], Vivek M. Prabhu[*a], Ashwin Rao[a], Eric K. Lin[a], Sushil K. Satija[b], Karen Turnquest[c], Wen-li Wu[a]

[a]Polymers Division, National Institute of Standards and Technology, Gaithersburg, MD
[b]Center for Neutron Research, National Institute of Standards and Technology, Gaithersburg, MD
[c]SEMATECH, 2706 Montopolis Dr, Austin, Texas 78741

## ABSTRACT

An understanding of acid diffusion-reaction in chemically amplified photoresists during the post-exposure bake (PEB) is critical for both critical dimension (CD) and line edge roughness (LER) control. Despite its importance, there remains insufficient understanding of the diffusion-reaction process. This is due in part to the complex interplay between diffusion and reaction where the deprotection of the resin modifies the local acid diffusivity which in turn changes the rate of deprotection. Here, we report the direct measurement of the reaction diffusion front at a model line edge from neutron reflectivity and Fourier transform infrared spectroscopy measurements. The photoacid generator size influences the reaction extent and breath of the deprotection profile. A larger photoacid results in a sharper deprotection profile and a shorter reaction length. Under the same post-exposure bake time and temperature, the smaller photoacid leads to a much broader deprotection profile. These measurements illustrate the complexity of the reaction-diffusion process.

Keywords: Photolithography, chemically amplified photoresists, diffusion, neutron reflectivity, line edge roughness

## INTRODUCTION

In the photolithographic process, there are three key steps to the quality of the final features: exposure, post-exposure bake (PEB), and development. The quality of the optical image is generally the primary factor,[1] but it is increasingly difficult to meet design specifications with only improvement in the aerial image quality.[2] Line edge roughness (LER) control to $3\sigma$ of less than 5 nm seems limited by the resist itself.[2] Thus, fundamental understanding of the processes during the PEB and development steps could lend insight into potential routes to LER improvement. Here, the coupling of acid diffusion and catalytic reaction during the PEB is explored in detail. These processes form the latent chemical image in the resist, which determines the final quality of the developed feature.

Measurements of the reaction-zone between unexposed and exposed regions can be interpreted with lithographic techniques and reaction-diffusion models. However, the fundamental mechanisms of the reaction-diffusion process are difficult to ascertain from lithographic measurement. Thus, recently simplified model systems based upon formation of acid rich and acid free regions (multilayer or bilayer) have been utilized to understand the deprotection process from a fundamental perspective.[3-7] One key result is that acid diffusion is strongly dependent upon the local environment where there is an order of magnitude difference in the diffusivity of the photoacid within protected and deprotected poly(hydroxystyrene) based resists.[3, 4] The acid diffusion is generally cited as the primary source of image spreading or blurring,[8] however the catalytic efficiency of the photoacid can also lead to blurring.[4] Nonetheless, feature quality is significantly affected by the acid diffusion during processing.[9-11] In particular, the shape of the deprotection at the line edge is suspected to be a determining factor of line edge roughness (LER).[5, 12]

In the present case, a bilayer geometry is utilized to follow the reaction-diffusion process. This results in highly idealized step acid profile with width less than 2 nm.[13] Previously the influence of the post-exposure bake on the reaction front profile in a model 248 nm resist was investigated for a single photoacid generator (PAG).[5, 12] For these

[§] Official contribution of the National Institute of Standards and Technology; not subject to copyright in the United States

Advances in Resist Technology and Processing XXIII, edited by Qinghuang Lin
Proc. of SPIE Vol. 6153, 615316, (2006) · 0277-786X/06/$15 · doi: 10.1117/12.656464

phenolic resists, increasing the breath of the deprotection front results in increased LER.[3, 9, 14, 15] However, resists for the current 193-nm node are methacrylate based[16] and are expected to be used into the 45 nm node with immersion lithography.[17] The change in the resist chemistry between these nodes completely alters the development mechanism.[18] Thus, how acid diffusion / reaction during the PEB changes is an outstanding question with significant processing implications.

The reaction front profile in poly(methyladamantyl methacrylate) (PMAdMA), a model 193 nm polymer, is measured by combining neutron reflectivity (NR) with Fourier transform infrared spectroscopy (FTIR). Previously for 248-nm resists,[5] the complete removal of the deprotection products allowed for direct measurements of the deprotection reaction with NR. For the PMAdMA system, the deprotection products are significantly less volatile. FTIR quantifies the total deprotection extent and residual methylene adamantane. The FTIR data are used to determine the deprotection profiles from NR. The effect of photoacid generator (PAG) size on the reaction front profile is examined for a series of ionic PAGs.

## EXPERIMENTAL METHODOLOGY[#]

### 1. Materials

Poly(methyladamantyl methacrylate) (PMAdMA) ($M_n$ = 8800 g/mol, PDI = 1.18) was obtained from DuPont Electronic Materials. PMAdMA films were spin cast from toluene solution. Silicon wafers (76 mm diameter, 700 μm thick) primed with hexamethyldisilazane (HMDS) were used as substrates. The preparation of the bilayer necessitates the formation of a sharp interface between the two layers after spin coating both layers. The acid-feeder layer examined consists of poly(4-hydroxystyrene) (PHS) (DuPont Electronic Materials, $M_n$ = 8000 g/mol) containing 5 % by mass of a photoacid generator (PAG). Three different PAGs were examined: triphenylsulfonium triflate (TPS-Tf), triphenylsulfonium perfluorobutanesulfonate (TPS-PFBS), and di(*tert*-butylphenyl)iodonium perfluorooctanesulfonate (DTBPI-PFOS). Vinyl deuterated (d3-)PHS (Polymer Source) was used in the acid feeder to determine the partitioning of the methylene adamantane reaction byproduct for some cases.

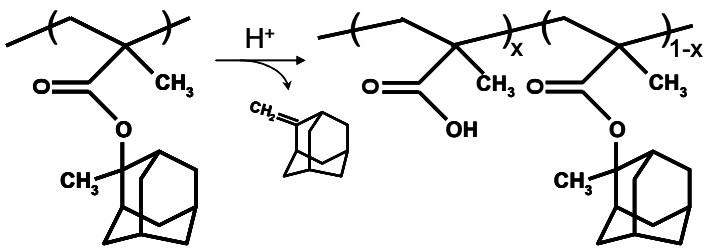
Details on the preparation of bilayer films are provided elsewhere.[12] Films are post apply baked (PAB) at 130 °C to remove residual solvent. The bilayer is exposed to broadband UV radiation (300 mJ/cm$^2$) to activate the PAG. A constant post exposure bake (PEB) temperature of 130 °C is used for the acid-diffusion deprotection reaction. To determine the surface roughness of the bilayers, the acid feeder layer and the deprotected portion of the bottom layer are developed with a 0.26 N tetramethylammonium hydroxide (TMAH) (Aldrich).

### 2. Methods

Neutron reflectivity (NR) measurements were performed at the Center for Neutron Research (NCNR) on the NG-7 reflectometer at the National Institute of Standards and Technology (Gaithersburg, MD) in the following configuration: wavelength ($\lambda$) = 4.768 Å and wavelength spread ($\Delta\lambda/\lambda$) = 0.025.[§] The large difference in hydrogen content between PHS and PMAdMA allows for the bilayer to be resolved with NR. The hydrogen density of the PMAdMA layer is significantly reduced upon deprotection and loss of methylene adamantane (by-product), thus providing a route for obtaining the deprotection profile through the film thickness.

[#] Certain commercial equipment and materials are identified in this paper in order to specify adequately the experimental procedure. In no case does such identification imply recommendations by the National Institute of Standards and Technology nor does it imply that the material or equipment identified is necessarily the best available for this purpose.

[§] The data throughout the manuscript and the figures are presented along with the standard uncertainty (±) involved in the measurement based on one standard deviation




*Scheme 1. Acid catalyzed thermally activated deprotection of PMAdMA.*

The characterization of deprotection reaction (see scheme 1) and methylene adamantane (MA) residual is made with a Nicolet NEXUS 670 Fourier transform infrared (FTIR) spectrometer equipped with a liquid nitrogen cooled MCT/A detector. Double-side polished, with orientation <100> and (1 to 50) ohm-cm resistance silicon wafers were used to minimize substrate absorbance. The data are collected in transmission mode with the OMNIC online-data acquisition software. A wave number resolution of 8 $cm^{-1}$ was used and the data were averaged over 128 scans to improve the signal-to-noise ratio. With this resolution, the interference fringes produced by the double reflection of silicon wafer surfaces can be greatly reduced without losing the details of spectroscopic features. The melting point (130 $^oC$) and boiling point (203 $^oC$) of MA limit its volatility at ambient conditions. The quantification of deprotection reaction degree is based on the bending vibration mode of $CH_3$ (1360 $cm^{-1}$) in the protecting MA group of PMAdMA. This band completely disappears and leaves a flat baseline in the IR spectra if all the protected MA groups are reacted. The advantage of choosing this band is that it provides an absolute value of deprotection reaction and allows the discrimination of the free MA or residual MA from the protected MA group. The quantification of MA residual level is based on the stretching vibration of H-C(=C) (3065 $cm^{-1}$) in the free MA molecule. This band is at lower wavenumbers from the H-C(-C) vibration (usually <3000 $cm^{-1}$), which makes it possible to quantify the MA content accurately. The integrated composition of the film determined from FTIR is then used to decompose the $Q_c^2$ profile obtained from neutron reflectivity to the deprotection level and concentration of methylene adamantane.

## RESULTS AND DISCUSSION

The acid reaction-diffusion at a model line edge is quantified through the combination of neutron reflectivity (NR) and FTIR. A typical NR profile for a bilayer consisting of an acid-feeder layer and PMAdMA is shown in Figure 1. The reflectivity is shown as a function of the momentum transfer vector, $q = 4\pi / \lambda \sin(\theta)$. The reflectivity results from the interference of reflected neutrons between the substrate and film and provides detailed information with respect to the neutron scattering length density profile. This profile is modeled by a series of slabs with varying neutron scattering length density and absorbance coefficients. These density profiles are presented in units of $Q_c^2$ as a function of distance (Z) through the film. $Q_c^2$ is a scattering length density, with dimensions $Å^{-2}$, and is proportional to the average atomic scattering length, b ($Q_c^2 = 16\ \pi Nb$), where N is the number of nuclei.

To determine the deprotection profile, the routine begins with the best fit of the NR data that is physically realistic. Here the neutron scattering length density ($Q_c^2$) of the PMAdMA, methylene adamantane (MA), and fully deprotected PMAdMA are used as limits (see Table 1). The interfacial width between the PHS and PMAdMA layer was determined by using isotopic substitution: a vinyl (d3) deuterated PHS replaces the fully protonated PHS. The width is independent of annealing and does not increase appreciably upon PEB. Upon deprotection, some of the residual methylene adamantane is trapped in the PHS layer (less than 2 % by volume of residual MA). With these considerations in place, we can move forward to begin to fit the reaction front profile for the bilayers from the NR and FTIR data. The interfacial width between the PHS and this layer is defined from the isotopic substitution measurements as (2 to 3) nm. The thickness and $Q_c^2$ for an intermediate layer between PHS and PMAdMA, the thickness of the PMAdMA layer and interfacial width between intermediate layer and the PMAdMA are allowed to vary to best fit the NR data based upon a least squares approach.[19] As an example, the fit for a bilayer containing 5 % TPS-PFBS in PHS on top of PMAdMA with 15 s PEB at 130 °C is shown in Figure 1. The profile from this least-squares fit is well representative of the NR data. However, small changes to the $Q_c^2$ profile do not significantly influence the quality of the fit. Due to the relatively small contrast change between the PMAdMA and its deprotected analog, this could lead to significant uncertainty in the extracted deprotection profile. However, the additional data from FTIR limits the potential variation

in the $Q_c^2$ profile to fit the NR data. For the least squares fit profile in Figure 1, the calculated profile does not agree with the compositions from FTIR – the residual MA concentration is too low to match with the FTIR. To increase the methylene adamantane, the $Q_c^2$ of the intermediate layer is decreased slightly and then the thickness of the intermediate and PMAdMA layer and interfacial width between intermediate layer and the PMAdMA are allowed to vary to best fit the NR data based upon a least squares approach. This new fit profile is then subjected to the same comparison with the FTIR data and the process is repeated until the fit agrees with the FTIR data within 3 %. The change in the profile shape between the least squares fit and the best fit including the FTIR data is generally minimal as illustrated in Figure 1b, but is important to extract the most accurate deprotection profile from the NR data.

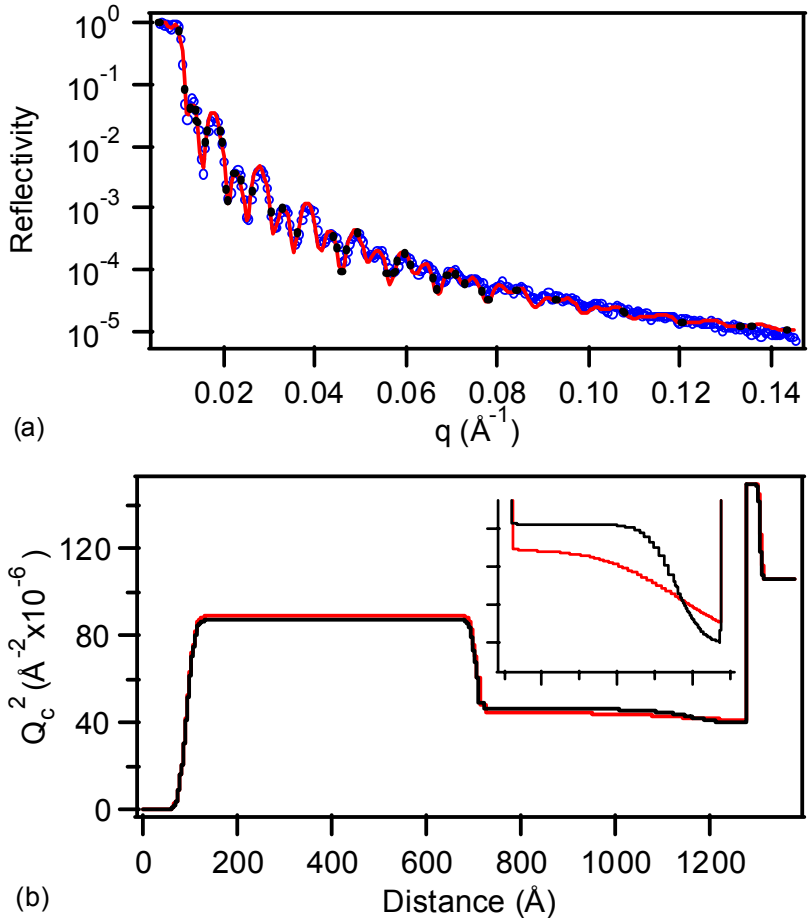



*Figure 1. Typical NR profile for a bilayer sample. Fits of the reflectivity data (○) based upon best fit from least squares algorithm (dashed line) and when considering FTIR data (solid line). The inset in (b) illustrates the difference between these profiles. The fit of the data is nearly indistinguishable as shown in (a).*

The deprotection profiles determined from the combination of NR and FTIR data using TPS-PFBS for the PAG in the acid feeder are shown in Figure 2 as a function of PEB time. For the smallest PAG examined, the photoacid rapidly diffuses through the MAdMA receiving layer, deprotecting as it moves through the film. Greater than 40 % of the PMAdMA is deprotected 60 nm away from the initial photoacid front after only 8 s PEB at 130 °C. This temperature is higher than generally used for processing methacrylate-based resists. The elevated temperature volatilizes a substantial portion of the MA produced, which leads to improved resolution of the deprotection. As the PEB time is increased further, more deprotection occurs. It is interesting to note that the width of the reaction diffusion front from the TPS-Tf is similar to the pitch of the features imaged at 193 nm. However for this model system, no base quencher has been utilized and the model resin is a homopolymer. The influence of both of these mitigating factors on the reaction

diffusion front profile is a topic of future work. These bilayer films are removed entirely when developed with 0.26 N TMAH .

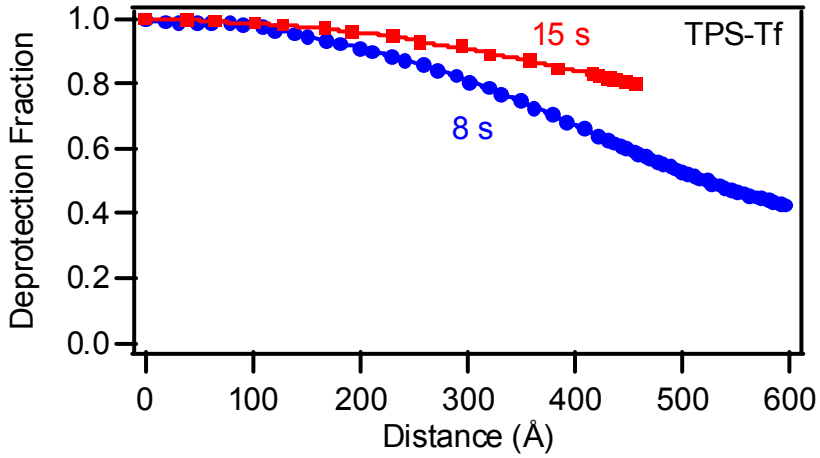



*Figure 2. Deprotection profiles using TPS-Tf as PAG with PEB at 130 °C for (●) 8 s and (□) 15 s. Lines are resultant from the fits; symbols are added to the curves for clarity in distinguishing conditions.*

As the photoacid counterion size is increased from Tf to PFBS, the diffusion coefficient for the photoacid decreases.[3] This results in a sharper deprotection front from the model line edge as shown in Figure 3. However, the profiles have significant 'tailing' where there is substantial background deprotection far into the film. Additionally, the front propagates rapidly into the film after 8 s PEB, but only a minor increase in deprotection is observed when the PEB time is doubled. Clearly there is either a significant change in the photoacid diffusivity within the deprotected regions or the catalytic lifetime of the photoacid is limited. Experiments described elsewhere in these proceedings confirm that the diffusion coefficient is strongly dependent upon the local deprotection composition. The photoacid diffusivity with the methacrylic acid rich regions formed by deprotection appears to be depressed by orders of magnitude in comparison to the fully protected analog.[20] This difference in diffusivity is much greater than that observed in phenolic resists.[4] Unlike for the TPS-Tf, development of these films yields residual films. The depth of the material removed is illustrated by the dashed lines in Figure 3. The solubility switch for the PMAdMA appears to be approximately 40 % deprotection. This is also consistent with the data in Figure 2 where the films exhibit deprotection greater than 40 % throughout.

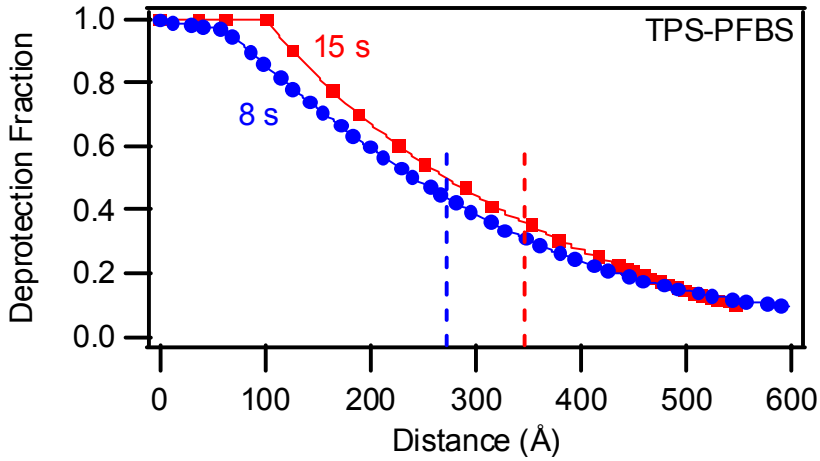



*Figure 3. Deprotection profiles using TPS-PFBS as PAG with PEB at 130 °C for (●) 8 s and (□) 15 s. Solid lines are resultant from the fits; symbols are added to the curves for clarity in distinguishing conditions. The dashed lines correspond to the depth into which the partially deprotected PMAdMA is removed by 0.26 N developer.*

Further increasing the PAG size to DTBPI-PFOS slows the photoacid diffusion and creates a much sharper front in comparison to both TPS-PFBS and TPS-Tf as shown in Figure 4. Similar to the observations using TPS-PFBS, the deprotection front rapidly progresses into the film and minimal further front propagation occurs with increased PEB time. In fact after 15 s PEB, the front appears to stagnate with nearly identical profiles between 15 s and 60 s PEB. The only difference at extended times is the increase in background deprotection. This behavior is consistent with the acid diffusivity being strongly dependent upon local environment. The PMAA can interact strongly with ionic species, leading to reduced diffusivity similar to that observed for phenolic resists.[4] Unlike phenolic resists, the deprotection reaction is not autocatalytic.[21] Thus, the deprotection front does not further propagate at long times apparently due to the combination of decreased acid diffusivity in the presence of high deprotection (MAA) levels and the nature of the deprotection reaction (non-autocatalytic). The dashed vertical lines in Figure 4 illustrate the development depth into the model bilayers with 0.26 N TMAH. Note that the change in dimensions is identical between samples with PEB > 15 s. This is due to a constant solubility switch for the system of 40 % deprotection.

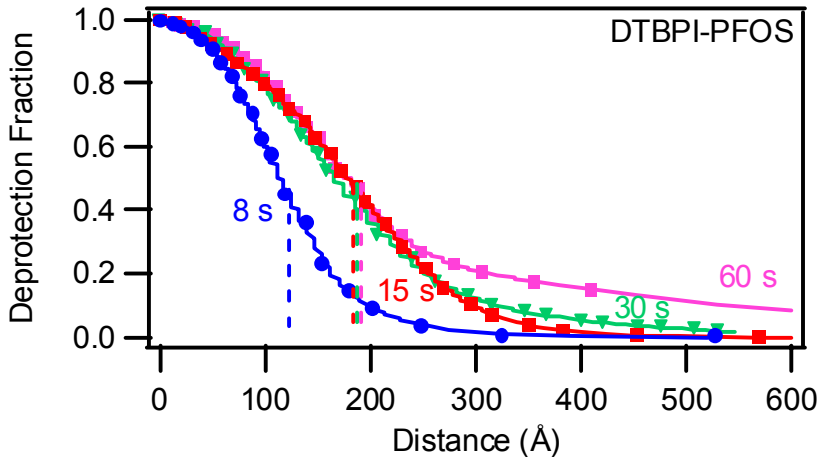



*Figure 4. Deprotection profiles using DTBI-PFOS as PAG with PEB at 130 °C for (●) 8 s, (□) 15 s, (▼) 30 s, and ( ■ ) 60 s. Solid lines are resultant from the fits; symbols are added to the curves for clarity in distinguishing conditions. The vertical dashed lines correspond to the developed thickness using 0.26 N TMAH.*

From a processing perspective, these contrasting cases favor a larger PAG due to smaller diffusion length with equivalent processing – this will limit changes in the critical dimensions and image blur. The shorter diffusion length with increasing PAG size is consistent with previous indirect measurements.[3] These measurements have enabled a quantitative distinction between photoacid size by avoiding some necessary complexities to be addressed in the future, for instance the effect of base additives and comonomer content. The latter provides a necessary step to understand photoresists which are co and terpolymers.

## CONCLUSIONS

The line edge deprotection profile of a model 193 nm photoresist (PMAdMA) was examined using neutron reflectivity. Three different photoacid generators were examined; the larger the photoacid, the shorter the deprotection depth into the PMAdMA film and the sharper the deprotection profile. In the case for the PFOS system, where a large range in post-exposure bake times were possible, the reaction front spatial extent appears self-limited. While acid diffusion is expected to occur, a mechanism to account for a ceased front advancement transitioning into a background level of reaction is required. Data from experiments performed to understand the influence of amine base additives and comonomer content to quantify the influence on the spatial extent of the reaction front are forthcoming. These results in combination with dissolution behavior should provide needed quantitative measurements to understand the materials sources of line-edge roughness.

## ACKNOWLEDGEMENTS

This work was supported by SEMATECH under Agreement #309841 OF. The authors acknowledge Jim Sounik and M. Sheehan at DuPont Electronic Polymers for providing the polymers used in this study.

## REFERENCES

1. Levinson HJ, Arnold WH. Focus: The critical parameter for submicron lithography. J Vac Sci Techn B 1987; 5:293-298.

2. Pawloski A, Acheta A, Lalovic I, La Fontaine B, Levinson H. Characterization of line-edge roughness in photoresist using an image fading technique. Proceedings of the SPIE - The International Society for Optical Engineering 2004; vol.5376, no.1:414-425.

3. Hinsberg WD, Houle FA, Sanchez MI, Wallraff GM. Chemical and physical aspects of the post-exposure baking process used for positive-tone chemically amplified resists. Ibm Journal of Research and Development 2001; 45(5):667-682.

4. Houle FA, Hinsberg WD, Morrison M, Sanchez MI, Wallraff G, Larson C, Hoffnagle J. Determination of coupled acid catalysis-diffusion processes in a positive-tone chemically amplified photoresist. J Vac Sci Techn B 2000; 18(4):1874-1885.

5. Lin EK, Soles CL, Goldfarb DL, Trinque BC, Burns SD, Jones RL, Lenhart JL, Angelopoulos M, Willson CG, Satija SK, Wu WL. Direct Measurement of the Reaction Front in Chemically Amplified Photoresists . Science 2002; 297:372-375.

6. Schlegel L, Ueno T, Hayashi N, Iwayanagi T. Determination of acid diffusion in chemical amplification positive deep ultraviolet resists. J Vac Sci Techn B 1991; 9(2):278-289.

7. Zuniga M, Wallraff GM, Neureuther AR. Reaction diffusion kinetics in deep-UV positive-tone resist systems. Proceedings of the SPIE - The International Society for Optical Engineering 1995; 2438:113-124.

8. Wallraff GM, Hinsberg WD. Lithographic Imaging Techniques for the Formation of Nanoscopic Features. Chem Rev 1999; 99:1801-1821.

9. Kim JH, Kim YH, Chon SM, Nagai T, Noda M, Yamaguchi Y, Makita Y, Nemoto H. Influence of acid diffusion length on line edge roughness in KrF photoresists. Journal of Photopolymer Science and Technology 2004; 17(3):379-384.

10. Schmid GM, Stewart MD, Singh VK, Willson CG. Spatial distribution of reaction products in positive tone chemically amplified resists. J Vac Sci Techn B 2002; 20(1):185-190.

11. Stewart MD, Tran HV, Schmid GM, Stachowiak TB, Becker DJ, Willson CG. Acid catalyst mobility in resist resins. Journal of Vacuum Science & Technology B 2002; 20(6):2946-2952.

12. Jones RL, Prabhu VM, Goldfarb DL, Lin EK, Soles CL, Lenhart JL, Wu WL, Angelopoulos M. Correlation of the reaction front with roughness in chemically amplified photoresists. Washington D.C.: American Chemical Society, 2004: 86-97.

13. Goldfarb DL, Angelopoulos M, Lin EK, Jones RL, Soles CL, Lenhart JL, Wu WL. Confinement effects on the spatial extent of the reaction front in ultrathin chemically amplified photoresists. Journal of Vacuum Science & Technology B 2001; 19(6):2699-2704.

14. Houle FA, Hinsberg WD, Sanchez MI. Acid-base reactions in a positive tone chemically amplified photoresist and their effect on imaging. Journal of Vacuum Science & Technology B 2004; 22(2):747-757.

15. Nakamura J, Ban H, Tanaka A. Influence of Acid Diffusion on the Lithographic Performance of Chemically Amplified Resists. Japanese Journal of Applied Physics Part 1-Regular Papers Short Notes & Review Papers 1992; 31:4294-4300.

16. Ito H. Chemical Amplification Resists for Microlithography. Adv Polym Sci 2005; 172:37-245.

17. Dammel RR, Houlihan FM, Sakamuri R, Rentkiewicz D, Romano A. 193 nm immersion lithography - Taking the plunge. Journal of Photopolymer Science and Technology 2004; 17(4):587-601.

18. Hinsberg W, Houle FA, Lee SW, Ito H, Kanazawa K. Characterization of reactive dissolution and swelling of polymer films using a quartz crystal microbalance and visible and infrared reflectance spectroscopy. Macromolecules 2005; 38(5):1882-1898.

19. Ankner JF, Maikrzak CF. SPIE 1992; 1738:260.

20. Kang S, Prabhu VM, Vogt BD, Lin EK, Wu WL, Turnquest K. Copolymer fraction effect on acid catalyzed deprotection reaction kinetics in model 193 nm photoresists. Proceedings of the SPIE - The International Society for Optical Engineering 2006; 6153-138:in this volume.

21. Paniez PJ, Gally S, Mortini BP, Rosilio C, Sassoulas P-O, Dammel RR, Padmanaban M, Klauck-Jacobs A, Oberlander JE. Thermal phenomena in acrylic 193-nm resists. Proceedings of the SPIE - The International Society for Optical Engineering 1999; 3678:1352-1363.